

## OPTICAL COATINGS OF CVD-TRANSITION METAL OXIDES AS FUNCTIONAL LAYERS IN "SMART WINDOWS" AND X-RAY MIRRORS

K. A. Gesheva\*, T. Ivanova, F. Hamelmann<sup>a</sup>

Central Laboratory of Solar Energy and New Energy Sources - BAS,  
Blvd. "Tzarigradsko chaussee" 72, 1784 Sofia, Bulgaria

<sup>a</sup>University of Bielefeld, Faculty of Physics, D-33615 Bielefeld, Germany

The paper presents the recent study on the technology and investigation of thin metal oxide films based on transition metals, such as W and Mo. Defined is the application aspect of the research, by describing the optical systems based on these films, namely the electrochromic device and the X-ray mirror. Results on the optical absorption in the films are presented, and discussed by the specific structure of these materials. Electrochromic measurements of the MoO<sub>3</sub>, as well as of mixed oxide films based on W and Mo are more in details presented. A device based on mixed oxide films as working electrode is developed and its electrochromic functioning evidenced by the voltammograms, coloration efficiency and optical modulation is described.

(Received April 25, 2005; accepted after revision May 26, 2005)

*Keywords:* Transition metal oxides, Optical properties, Electrochromic behaviour

### 1. Introduction

The recent research results presented in the paper are focused on the technology and investigation of electrochromic transition metal oxide thin films based on tungsten and molybdenum oxides. These materials are interesting from the point of view of basic science and technology. An electrochromic material is able to change its optical properties when a small voltage pulse is applied across the material [1,2]. This phenomenon is supposed to be reversible if the polarity of the voltage is changed the original state should be recoverable. These properties are exclusively interesting especially if regarding their applications such as elements for information displays, shutters for the light, smart windows, antidazzling mirrors, thermal radiators, etc [3-5]. It is important to note that even if a single thin film exhibits electrochromism, it should be a part of an optical system with a special construction in order to exhibit the effect. This system should allow the application of a voltage. The optical modulation (the change in the transmittance in the two modes, colored and bleached) is connected with the differences in the electron density of the oxides. So, the electrodes necessary to make the electrical contacts should permit injection or extraction of electrons.

The characteristic properties of transition metal oxides are mainly determined by their specific band structure and electron distribution. They possess d-electrons, which create d-band partially overlapping s-band. The d-band provokes the interesting chemical, physical and optical properties of transition metal oxides.

Molybdenum oxide films show well pronounced electrochromic effect [6,7] and many properties, which are similar to the mostly investigated W oxide films. MoO<sub>6</sub> octahedron is the building unite of the specific layered structure of MoO<sub>3</sub>, in which one oxygen is unshared, two oxygen atoms are common to two octahedral, and three oxygens are in part-shared edges and common to three octahedral. This layered structure is usually referred to as the  $\alpha$  phase. The internal interaction among atoms is dominated by ionic and covalent forces, but the sublayers pair is

---

\* Corresponding author: kagesh@phys.bas.bg

interacted by weak van der Waals forces [8]. This structure gives opportunity for injection of different donor ions into interlayered spaces and favors EC properties. From other hand, the metastable monoclinic  $\beta$  - phase has a cubic  $\text{ReO}_3$  - like structure, consisting of three-dimensional rows of shared  $\text{MoO}_6$  octahedra [9]. The open crystalline structure of Mo oxide makes this material very good host material for ions like Li, protons, K, Na. This property makes this material a good electrochromic material.

Another application for Mo and W based transition metal oxides are multilayers as mirrors for the extreme ultraviolet radiation (EUV, wavelength between 2 and 50 nm). Such multilayers can be obtained by alternated deposition of two materials with different complex refraction index and a double layer thickness in the range of the EUV wavelength [10]. Because of the importance for "next generation" chip technology (the so called extreme ultraviolet lithography EUVL), a lot of studies have been done for the 13 nm wavelength. At this wavelength metallic molybdenum/silicon multilayers provide the highest reflectivity, up to 70% [11]. However, such multilayers need high purity and extremely low interface roughness to obtain a high reflectivity and are usually produced by PVD methods such as electron beam evaporation or magnetron sputtering [12]. Carbon and oxygen impurities will dramatically decrease the reflectivity at this wavelength. For shorter wavelengths, in the "water window" between the carbon and oxygen absorption edges at 4.4 and 2.4 nm, oxygen is transparent. Furthermore, metal oxides form very stable interfaces and diffusion barriers in multilayered structures, a very low interface roughness with small roughness correlation lengths, important to deposit multilayers with a high number of periods and ultrathin layers. This is another advantage of oxide multilayers [13].

Recently deposited multilayer system of  $\text{WO}_3/\text{SiO}_2$  has shown that in combination with thin  $\text{SiO}_2$  films, multilayers with tungsten oxide layers with less than one nanometer thickness showed excellent periodicity even without in-situ thickness control and a very low roughness of 0.3 nm. The results suggest, that multilayers with an even higher number of periods, suitable as mirrors for EUV radiation, are possible to deposit with oxygen plasma enhanced CVD. The interface roughness may be further reduced by variation of the deposition parameters (bias voltage, oxygen flow, plasma power).

## 2. Experimental

It is established that  $\text{MoO}_3$  films are successfully obtained in the temperature range of 150-200 °C by atmospheric CVD process. Experiments with increasing the deposition temperature above 200 °C (300 and 400 °C) showed that there was no film deposits, nevertheless there were enough carbonyls vapors in the reactor, because powder and deposits on reactor walls were registered. This proves that CVD process for  $\text{MoO}_3$  film deposition requires lower  $T_{\text{deposition}}$  compared with the analogical process for  $\text{WO}_3$  films, which were successfully deposited in the temperatures of 200 to 400 °C [14]. Details of CVD deposition can be found elsewhere [15,16]. The film thickness was in the range of 320-400 nm for the low-temperature set of samples and 120-240 nm for the 200 °C-set of samples. The two kinds were grown for one and the same deposition time. The two sets of samples in as deposited state differ in their color. The samples of the lower-temperature look bluish, when the 200 °C-set of samples are yellowish.

Films of  $\text{MoO}_3$ ,  $\text{WO}_3$  and mixed  $\text{MoO}_3$ - $\text{WO}_3$  oxide were deposited on conductive glass (Donnelly type  $\text{SnO}_2$ :Sb) and Si substrates, by atmospheric pressure pyrolytic decomposition of the corresponding hexacarbonyls,  $\text{W}(\text{CO})_6$ ,  $\text{Mo}(\text{CO})_6$ , or their suitable physical mixtures. The mixed precursor was prepared in a ratio of 1:4 in favor of the  $\text{W}(\text{CO})_6$ . The vapor source temperature was 90°C. The chosen ratio of the flow rates of argon through the vapor source to oxygen was 1:32 to supply a rich of oxygen environment in the CVD reactor. The deposition temperature was 200 °C. This was the crossing point of the deposition temperatures for the three kinds of metal oxide film [16]. The deposition time was kept constant (40 min) and because of the different growth rates the film thickness was about 300 nm for  $\text{MoO}_3$ , 120 nm for  $\text{WO}_3$  and 400 nm for mixed oxide films. Apparently, the presence of two components in the chemical reaction changes the growth kinetics, leading to an increased growth rate of the mixed oxide films at temperature of 200°C, where  $\text{WO}_3$  grows very slowly.

The optical parameters of the MoO<sub>3</sub> films were deduced from the spectroscopic ellipsometric measurements carried out in the spectral region of 300 - 800 nm using Rudolph Research ellipsometer with PCSA configuration. The refractive index, N, and the extinction coefficient, k, were calculated for a single-layer/substrate optical system assuming that the films are a homogeneous medium.

Cyclic voltammetry experiments were performed in a standard three-electrode arrangement. The cell adopted had Pt as a counter electrode, and a saturated calomel (SCE) reference electrode. The sweeping potentials were provided by a Bank - elektronik Potentiostat, under computer control. The electrodes were immersed in an electrolyte of 1 mol/l LiClO<sub>4</sub> in propylene carbonate (PC) or 1M H<sub>2</sub>SO<sub>4</sub>+ 50% glycerine. To change the wavelength, a monochromator was installed in the system, permitting the color efficiency to be estimated over a large spectral range (400-800 nm).

By plasma-enhanced CVD, using tungsten hexacarbonyl W(CO)<sub>6</sub> as a precursor with an oxygen plasma for precursor decomposition and oxygen supply, thin films of WO<sub>3</sub> were deposited. In combination with SiO<sub>2</sub> (deposited from TEOS Si(OC<sub>2</sub>H<sub>5</sub>)<sub>4</sub>), multilayers with WO<sub>3</sub> single layer thickness of less than 1 nm and 40 periods have been produced with the PECVD equipment.

The in-situ soft X-ray measurement of the reflectivity, applied during the PECVD deposition, consists of a XPS X-ray source coated with carbon, which is emitting 4.4 nm radiation (carbon K-line). The source is mounted at 20° to the substrate. A proportional counter under the same angle of incidence detects the reflected radiation. The resulting reflectivity curves show an oscillating behaviour due to waves interference of reflected at the film/substrate interface and the film surface. The values of wavelength  $\lambda$  and angle of incidence  $\alpha$  determine the film thickness  $d$  for one period of oscillation, as given in first order by Bragg's law  $\lambda = 2d \cos\alpha$  [13]. This method gives information about surface roughness and film density, also. Due to the absorption of the film, this method is only useful for smooth films up to a thickness of 10 nm (for high absorbing metals) or 100 nm (for low absorbing materials like SiO<sub>2</sub>).

### 3. Results and discussion

First, MoO<sub>3</sub> films obtained at the lower deposition temperature was analyzed by UV-VIS spectroscopy. As it was mentioned, the two sets of films are visually different in their color. The 150 °C-deposited films are bluish in color, which is characteristic for substoichiometric MoO<sub>x</sub> and is connected with the presence of oxygen vacancies into the structural film order. The transparency of as deposited film at 150 °C is around 45% in the visible range and improving of the transmittance is observed after annealing. The 400 °C - annealed MoO<sub>3</sub> film has 78% transparency. The increase of transparency for the annealed MoO<sub>3</sub> films is suggested as due to the additional oxidation of the film and decrease of the number of oxygen defects in the material. For the second set of thin films, prepared at T<sub>deposition</sub>=200 °C, the optical transmittance increase from 35% for as deposited films up to 70% for 300 °C treated MoO<sub>3</sub> film. The annealed samples deposited at the increased oxygen content (Mo(CO)<sub>6</sub>/O<sub>2</sub>=1/34) have transparency around 80%.

The absorption coefficient for the different process temperatures is evaluated from the corresponding extinction coefficient. The spectral dependences are presented in Fig. 1. There is not a clear dependence on deposition temperatures below the absorption edge. The  $\alpha$  values remain smaller than  $5 \times 10^4 \text{ cm}^{-1}$  for wavelengths below the absorption edge. Approaching the absorption edge band to band electronic transitions take place and the absorption strongly increases, having higher values for the films, deposited at 200 °C. The shape of the curves is similar for T<sub>sublimator</sub>=70 and 80 °C and differs significantly only for T<sub>sublimator</sub> = 90 °C. For the latter two well-pronounced strong absorption bands appear. These peculiarities at energies below the absorption edge could be connected with proper type of defects giving states in the forbidden band gap. Similar optical absorption bands were observed by C. Julien et al. [17]. The observed bands were associated with defects of oxygen-ion vacancies in the MoO<sub>3</sub> film.

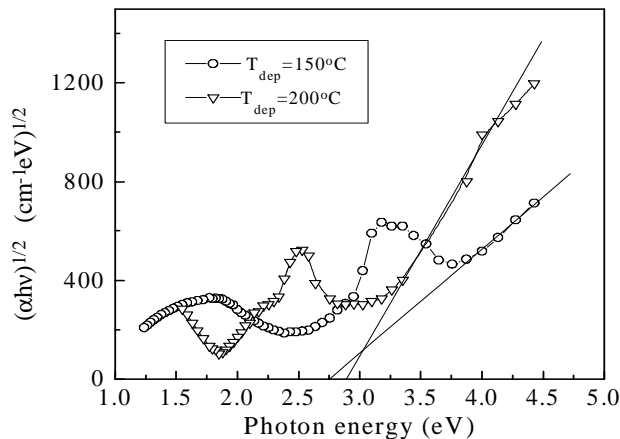


Fig. 1. Absorption coefficient as a function of the photon energy for the  $\text{MoO}_3$  films obtained at the  $T_{\text{deposition}}=150$  and  $200^\circ\text{C}$ .

The plot of  $(\alpha h\nu)^{1/2}$  versus  $h\nu$  determines the  $E_{\text{og}}$  values for films deposited at 150 and  $200^\circ\text{C}$  are presented on Fig. 1. It could be concluded that the sublimator temperature has no influence on the  $E_{\text{og}}$  value (2.91-3.04 eV) at  $T_{\text{deposition}}=150^\circ\text{C}$ , since the difference is in the range of the measurement accuracy. At  $200^\circ\text{C}$ , this difference is more noticeable. The values of the optical bandgap energy for all the films studied are within 2.76 - 3.14 eV, which is in agreement with the literature data [1, 18]. The observed  $E_{\text{og}}$  variation for different temperatures could be connected either with structure or thickness changes. In our experiments, however the deposition time was kept constant and different film thickness was obtained due to kinetics reasons. Because of the correlation between structure and film thickness, the influence of neither one on  $E_{\text{og}}$  values can be determined as dominant. The structure of the films as revealed by XRD, IR and Raman analysis is a mixture of amorphous and crystalline phases [19].

The transmittance in the visible wavelength range for  $\text{MoO}_3$ ,  $\text{WO}_3$  and mixed  $\text{MoO}_3\text{-WO}_3$  films from the comparison set varies within 60-80 % but comparison between the transmittance of the films cannot be directly made because of the different film thickness. Correspondingly, the values of reflectance are around 20%. After annealing  $\text{MoO}_3$  and  $\text{WO}_3$  films become more transparent, while transparency of the mixed oxide films decreases in the range of 400-750 nm and slightly increases towards longer wavelengths. The annealing does not have strong influence on the spectra of the  $\text{MoO}_3$  and  $\text{WO}_3$  films, while it leads to a noticeable decrease in the reflectance of the mixed  $\text{MoO}_3\text{-WO}_3$  oxide films.

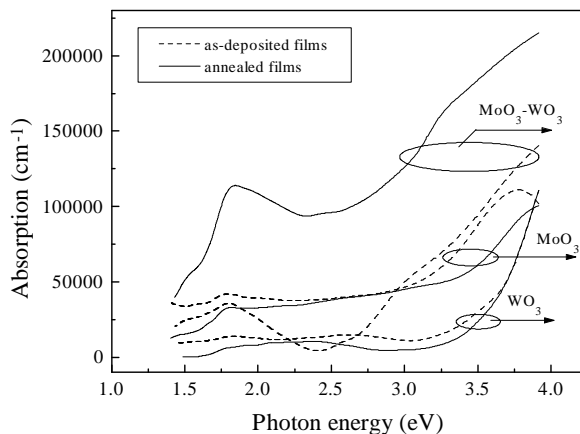


Fig. 2. Spectral dependence of the absorption coefficient ( $\alpha$ ) for  $\text{MoO}_3$ ,  $\text{WO}_3$  and  $\text{MoO}_3\text{-WO}_3$  for as-deposited (dotted line) and after  $400^\circ\text{C}$  (solid line) annealing films.

The absorption coefficient  $\alpha$  is determined by two independent methods, UV-VIS spectrophotometry and spectroscopic ellipsometry. Since the two dependences of  $\alpha$  well coincide, only the spectrophotometric results are shown in Fig. 2, where the absorption spectra of as-deposited and annealed films are presented. As it is seen, there is no maximum in the  $\text{WO}_3$  spectrum, it is almost plateau up to  $\sim 3$  eV. The small maximum at 1.7 eV in the spectrum of  $\text{MoO}_3$  transforms in the spectrum of mixed oxide film in a broad and deep maximum at 1.8 eV. In tungsten-molybdenum mixed oxide films Faughnan et al. [20] have found this absorption peak in the same energy range. After annealing, the absorption in pure metal oxides decreases, while in the mixed oxide films - significantly increases. We have noted after annealing a certain decrease of  $\alpha$  in these mixed oxide films when they are deposited on crystalline silicon substrates. This can be related to different film structure. The optical absorption for as-deposited films has, in addition, a second maximum around 2.75 eV, which in the case of  $\text{MoO}_3$  [21] appears at 2.5 eV. The enhanced absorption at energies below the absorption edge could be associated with proper type of defects in the metal oxides. Absorption bands in this energy range are also observed in [17] and they are associated with oxygen vacancies in  $\text{MoO}_3$  film.

$\text{MoO}_3$  films are almost transparent. After electrochemically done injections of small ions like  $\text{Li}^+$ ,  $\text{H}^+$  or  $\text{K}^+$  and electrons into films structure, their color changed to dark blue. The color modulation is proposed [2] to be connected with the double intercalation/deintercalation of ions and electrons and this reaction can be written as follows:



where  $\text{M}^+$  are small alkine ions. The present theories suggest that the optical absorption is provoked by reduction of  $\text{Mo}^{6+}$  levels to  $\text{Mo}^{5+}$  and the beginning of transfer among neighboring  $\text{Mo}^{5+}$  and  $\text{Mo}^{6+}$  sites.

The electrochemical experiments showed the differences between the two types of  $\text{MoO}_3$  films, deposited at 150 and 200 °C deposition temperatures. All samples revealed bigger current densities for 150 °C obtained  $\text{MoO}_3$  films. Fig. 3 presents the as deposited  $\text{MoO}_3$  films, obtained at 150 and 200 °C. The curves have no peculiarities and maximums what is an indication for amorphous and disordered structure. The basic peak due to Li injections is appeared at -1.37 V and the corresponding anodic peak (ion extractions) at -1.14 V. Fig. 4 shows CV curves for  $\text{MoO}_3$  films deposited at different oxygen content introducing into CVD reactor during the film growth. Differences appeared at the localizations of the ion intercalation peaks. They are observed at -1.37, -1.13 V for gas ratios 1/28 and 1/20, respectively. The cyclovoltamograms for the film obtained at highest oxygen revealed no clear cathodic peak. The anodic peaks are at -0.82, -1.12, -0.96 V for 1/20, 1/28 and 1/40.

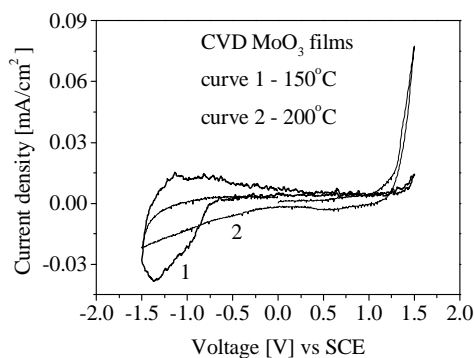


Fig. 3. CV curves of as deposited  $\text{MoO}_3$  films at 150 °C (1) and 200 °C (2).

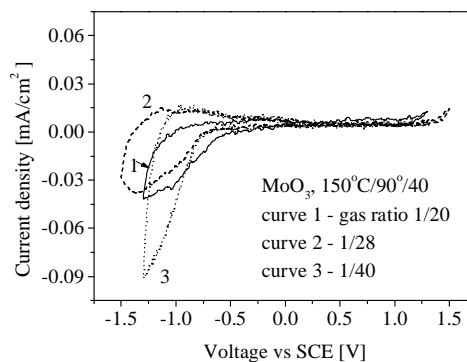


Fig. 4. CV curves of CVD as deposited  $\text{MoO}_3$  films at different gas ratios.

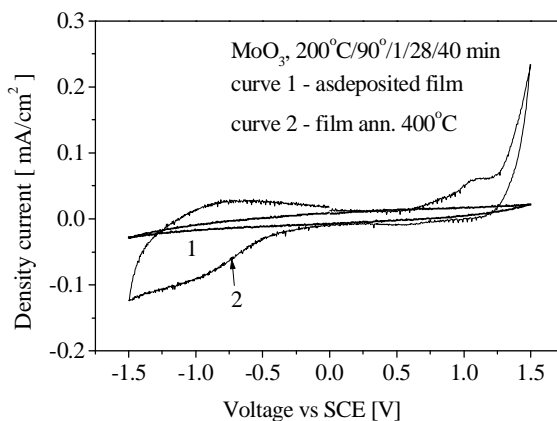


Fig. 5. CV curves of MoO<sub>3</sub> films, deposited at 200 °C in as deposited state and annealed at 400 °C.

Fig. 5 presents the electrochemical cycles of as deposited and annealed MoO<sub>3</sub> films obtained at 200 °C. Increasing the annealing temperatures leads to significant increase of current density. The diffusion coefficient of Li ions intercalated into electrochromic film can be determined using well known formula [22] and some data from electrochemical measurements as the concentration of active ions into the used electrolyte, sweep rate and the current density peak taken from the experimental CV curves. The estimated values for diffusion coefficient of Li ions in CVD MoO<sub>3</sub> films prepared at various technological conditions are presented in Table 1.

As can be seen the values of *D* varied depending on preparation parameters. C.G. Granqvist [1] reports values for diffusion coefficient for film with mixed orthorhombic and monoclinic structures in the range of 10<sup>-12</sup> - 5x10<sup>-12</sup> cm<sup>2</sup>/s, and for bulk orthorhombic MoO<sub>3</sub> the values are 10<sup>-11</sup> - 10<sup>-10</sup> cm<sup>2</sup>/s. Our results show that as deposited films from 150°C set and gas 1/28 and 1/40, *D* are closed to bulk material values. At these process parameters, the prepared films are amorphous with beginning of crystallization in orthorhombic modification as proved from previous XRD and Raman studies [19].

Table 1. Diffusion coefficient *D*<sub>Li</sub> for different MoO<sub>3</sub> films.

T <sub>deposition</sub> [°C]	Mo(CO) <sub>6</sub> /O <sub>2</sub>	T <sub>heating</sub> [°C]	<i>D</i> [cm <sup>2</sup> /s]
150	1/20	As deposited	2.56 × 10 <sup>-12</sup>
150	1/28	As deposited	1.60 × 10 <sup>-11</sup>
150	1/40	As deposited	1.06 × 10 <sup>-11</sup>
200	1/20	As deposited	1.50 × 10 <sup>-13</sup>
200	1/20	400 °C	2.20 × 10 <sup>-13</sup>
200	1/28	As deposited	5.29 × 10 <sup>-12</sup>
200	1/28	400 °C	6.76 × 10 <sup>-12</sup>
200	1/40	As deposited	4.90 × 10 <sup>-12</sup>

The color efficiency strongly depends on wavelength and on the changes in the optical density ( $\Delta OD$ ). It can be determined as  $CE = \Delta OD / Q$ , where  $\Delta OD$  is the change of the transmitted optical density at the wavelength of interest  $\lambda$ , due to the transfer of charge *Q* during a single-pass.

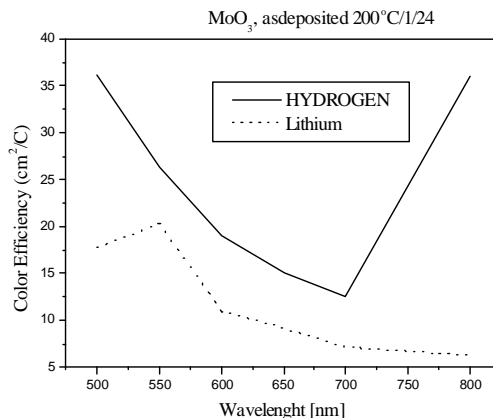


Fig. 6. Color efficiency of CVD – as-deposited  $\text{MoO}_3$  thin films, after  $\text{Li}^+$  and  $\text{H}^+$  insertion

Fig. 6 presents the estimated color efficiency of CVD molybdenum oxide films in the two kinds of electrolytes – lithium and hydrogen containing ions. The values of CE in case of hydrogen electrolyte are bigger, but although the glycerin is added in order to prevent the oxide film from destruction, destruction of CVD  $\text{MoO}_3$  film was observed after about 50 cycles.

The electrochromic characteristics of APCVD films of  $\text{MoO}_3$ ,  $\text{WO}_3$  and  $\text{MoO}_3\text{-WO}_3$  films were investigated. As can be seen from Fig. 7 the as deposited mixed films showed significant increase of current density in comparison with pure oxide films. Table 2 represented the estimated values for injected and extracted charge of CVD mixed oxide films.

From Fig. 7 and Table 2 can be proposed that there is an improvement of electrochromic properties of mixed film, annealed at  $400^\circ\text{C}$ . It is worth noting the sharp increase of the charge of  $\text{Mo}_x\text{W}_{1-x}\text{O}$  films. This fact proved the quality and applicability of these materials in EC devices. The absence of clearly pronounced peaks indicates amorphous material. The cathodic wave of  $\text{MoO}_3$  shows very weak peak at  $-0.42$  V. For pure  $\text{WO}_3$ , two clear peaks are distinguished at  $-0.46$  and  $-0.82$  V. For the mixed oxide, the cathodic maximum is localized at  $-0.73$  V.

Table 2. Determined charge values during electrochemical reaction. Q is in [ $\text{mC}/\text{cm}^2$ ] units.

Material	Annealing temperature	$Q_{\text{inserted}}$	$Q_{\text{extracted}}$
$\text{MoO}_3$	As deposited	31.57	30.36
	$400^\circ\text{C}/1$ hour	16.62	41.18
$\text{WO}_3$	As deposited	23.56	20.53
	$400^\circ\text{C}/1$ hour	39.20	31.40
$\text{Mo}_x\text{W}_{1-x}\text{O}_3$	As deposited	116.3	170.9
	$400^\circ\text{C}/1$ hour	195.59	204.51

Anodic peaks are at  $-0.2$  and  $-0.25$  V for  $\text{MoO}_3\text{-WO}_3$  and  $\text{WO}_3$ , respectively.  $\text{MoO}_3$  shows no anodic peak. After Li intercalation, the films are colored in deep blue and bleached after Li deintercalation. The most intensive coloring was observed for the mixed oxide films based on Mo and W. On Fig. 7 can be seen the electrochemical measurements of annealed films. The curves present more characteristic view especially for the mixed film, where well pronounced peaks are observed.

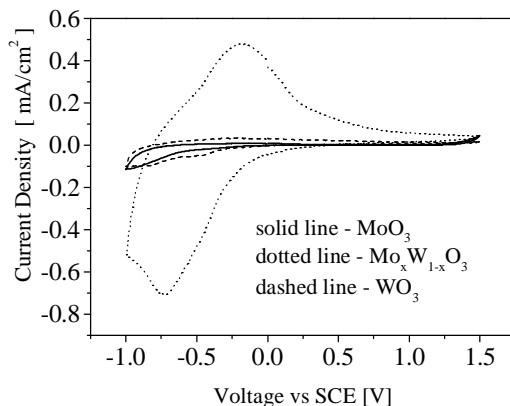


Fig. 7. Cyclic voltamograms of annealed at 400 °C films of MoO<sub>3</sub>, WO<sub>3</sub> and MoO<sub>3</sub>-WO<sub>3</sub>.

Table 3. Diffusion coefficients of Li ions in MoO<sub>3</sub>, WO<sub>3</sub> and Mo<sub>x</sub>W<sub>1-x</sub>O<sub>3</sub> films.

Material	T <sub>annealing</sub>	D [cm <sup>2</sup> /s]
MoO <sub>3</sub>	As-deposited	$6.76 \times 10^{-12}$
	400°C/1 hour	$5.3 \times 10^{-12}$
WO <sub>3</sub>	As-deposited	$9.6 \times 10^{-11}$
	400°C/1 hour	$2.25 \times 10^{-11}$
Mo <sub>x</sub> W <sub>1-x</sub> O <sub>3</sub>	As-deposited	$4.41 \times 10^{-10}$
	400°C/1 hour	$1.4 \times 10^{-11}$

Table 3 showed the values of  $D_{Li}$  for the three types of films. The best results are obtained for the mixed oxide system, suggesting easy and quick movement of lithium ions into their structure. Prior to the electrochemical measurements the as-deposited and annealed films had high transmittance (around 80-60%). The transmittance of the mixed MoO<sub>3</sub>-WO<sub>3</sub> films decreases rapidly after intercalation of Li ions into the film structure. The films were colored deep bluish and the transmittance values are under 10% for as-deposited and annealed (400°C) mixed films.

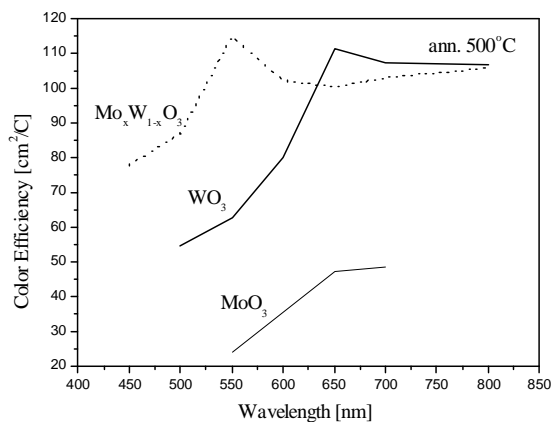


Fig. 8. Color efficiency values of CVD MoO<sub>3</sub>-WO<sub>3</sub> films, annealed at 300, 400 and 500 °C.

From the graphs on Fig. 8 is seen that the coloration efficiency of the mixed W/Mo based oxide films reaches the values for the reported as the best electrochromic material - WO<sub>3</sub>. It must be noted that the maximal value of the coloration efficiency of CVD MoO<sub>3</sub>-WO<sub>3</sub> films is located at the maximum of the solar spectrum (500-600 nm), which is another advantage of the mixed oxide films.

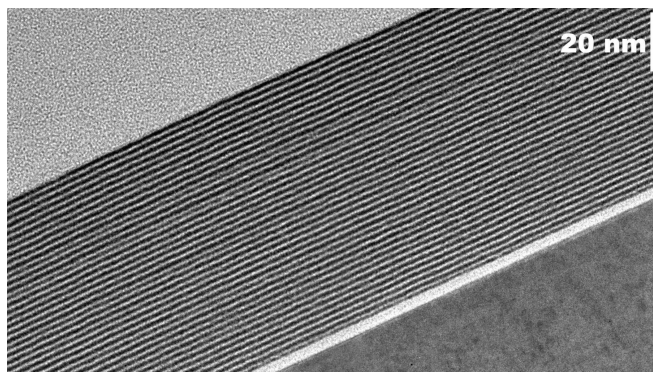


Fig. 9. TEM cross section of a WO<sub>3</sub>/SiO<sub>2</sub> multilayer,  $d = 2.1$  nm,  $n = 40$ .

Deposition of WO<sub>3</sub>/SiO<sub>2</sub> and MoO<sub>3</sub>/SiO<sub>2</sub> multilayers with a single layer thickness of about 4 nm using a radio frequency plasma results in extremely smooth interfaces with a roughness less than 0.2 nm. Calculations of the reflectivity of, for instance, WO<sub>3</sub>/SiO<sub>2</sub> showed that the peak reflectivity of the oxide based multilayer for water window wavelengths with a period less than 3 nm is much lower (about only 10%) than the reflectivity of the best EUV-reflector of Ti/C multilayer, but it has an increased value in a larger range – from about 3.4 to 2.3 nm, which covers most of the water window range. A beam reflected from such a system and having so short wavelength is very important and could be used for analyzing bioobjects with very small sizes. Besides, the real water, which is transparent in the water window range could be analyzed by such a beam, since the carbon is absorptive and could be detected easily. Such organic contaminations are real world problem for the water supply sources.

#### 4. Conclusion

Thin films from transition metal oxides successfully deposited by APCVD carbonyl process show excellent electrochromic behavior. The obtained color efficiencies meet the requirements of functional layers in practical electrochromic devices. The same types of films prepared by plasma enhanced CVD are applicable if combined with conventional metal oxides in optical systems – X-Ray mirrors. The multilayer system with tungsten oxide layers and thin SiO<sub>2</sub> films has shown showed excellent periodicity and a very low roughness of 0.3 nm.

#### Acknowledgements

The authors wish to thank to Assoc. Prof. Dr. A. Szekeres and her group for the valuable help with ellipsometric measurements and analysis. We acknowledge also the help of Prof. Dr. G. Poprikov and his group for providing us with equipment for electrochromic effect measurements.

#### References

- [1] C. Granqvist, "Handbook of Inorganic Electrochromic Materials", Elsevier Science, 1995
- [2] P. M. S. Monk, R. J. Mortimer, D. R. Rosseinsky, "Electrochromism: Fundamentals and Applications", VCH, 1995
- [3] M. Bell, J. P. Mathews, Solar Energy Mater. and Solar Cells **68**, 249 (2001).
- [4] A. Agrawal, J. Cronin, R. Zhang, Solar Energy Mater. Solar Cells **31**, 9 (1993).
- [5] U. Krasovec, A. Vuk, B. Orel, Solar Energy Mater. Solar Cells **73**, 21 (2002).
- [6] V. Sabhapathi, O. Hussain, P. Reddy, K. Reddy, S. Uthanna, B. Naidu, P. Reddy, Phys. Stat. Solidi (a) **148**, 167 (1995).
- [7] J. S. Cross, G.L. Schrader, Thin Solid Films **259**, 5 (1997).

- [8] F. Fereirra, T. Souza Cruz, M. C.A. Fantini, M.H.Tabacniks, S. de Castro, J. Morais, A. de Sierro, R. Landres, A. Gorenstein, *Solid State Ionics* **136 – 137**, 357 (2000).
- [9] W. M. R. Divigalpitiya, R. F. Frindt, S. R. Morrison, *Thin Solid Films* **188**, 173 (1990).
- [10] E. Spiller, *Appl. Phys. Lett.* **20**, 365 (1972).
- [11] U. Kleineberg, T. Westerwalbesloh, W. Hachmann, U. Heinzmann, J. Tümmeler, G. Ulm, S. Müllender, *Thin Solid Films* **433**, 230 (2003).
- [12] S. Braun, H. Mai, M. Moss, R. Scholz, A. Leson, *Jpn. J. Appl. Phys.* **41**, 4074 (2002).
- [13] F. Hamelmann, G. Haindl, J. Schmalhorst, A. Aschentrup, E. Majkova, U. Kleineberg, U. Heinzmann, A. Klipp, P. Jutzi, A. Anopchenko, M. Jergel, S. Luby, *Thin Solid Films* **358**, 90 (2000).
- [14] D. Gogova, K. Gesheva, A. Kakanakova-Georgieva, M. Surtchev, *Eur. Phys. J. Applied Physics* **11**, 167 (2000).
- [15] K. Gesheva, T. Ivanova, A. Iossifova, D. Gogova, R. Porat, *J. Phys.IV France* **9**, Pr8-53 (1999).
- [16] K. Gesheva, A. Szekeres, T. Ivanova, *Solar Energy Materials and Solar Cells* **76**, 563 (2003).
- [17] C. Julien, A. Khelfa, O. Hussain, G. Nazri, *J. Cryst. Growth* **156**, 234 (1995).
- [18] N. Miyata, T. Suzuki, R. Ohyama, *Thin Solid Films* **281-282**, 218 (1996).
- [19] T. Ivanova, K. Gesheva, A. Szekeres, A. Maksimov, S. Zaitzev, *J. Phys. IV France* **11**, Pr3-385 (2001).
- [20] B. W. Faughnan, R. S. Randall, *Appl. Phys. Lett.* **31**, 834 (1997).
- [21] Y. Wang, N. Herron, *J. Chem. Phys.* **95**, 525 (1991).
- [22] M. Habib, P. Glueck, *Solar Energy Materials* **18**, 127 (1989).